Immunity, Vol. 23, 7–18, July, 2005, Copyright ©2005 by Elsevier Inc. DOI 10.1016/j.immuni.2005.04.011

B-1a and B-1b Cells Exhibit Distinct Developmental Requirements and Have Unique Functional Roles in Innate and Adaptive Immunity to *S. pneumoniae*

Karen M. Haas, Jonathan C. Poe, Douglas A. Steeber, and Thomas F. Tedder*
Department of Immunology
Box 3010
Duke University Medical Center
Durham, North Carolina 27710

Summary

B-1a and B-1b lymphocytes were found to exhibit specialized roles in providing immunity to *Streptococcus pneumoniae* and differ dramatically in their developmental requirements. Transgenic mice overexpressing CD19 (hCD19Tg) generated B-1a cells and natural antibodies that provided protection during infection, while CD19-deficient ($CD19^{-/-}$) mice lacked B-1a cells, lacked natural antibodies, and were more susceptible to infection. By contrast, pneumococcal polysaccharide (PPS) immunization protected $CD19^{-/-}$ mice during lethal challenge, whereas hCD19Tg mice remained unprotected. This resulted from differences in the B-1b subset: the key population found to produce protective PPS-specific antibody in both wild-type and $CD19^{-/-}$ mice. Thus, $CD19^{-/-}$ mice generated B-1b cells and protective adaptive PPS-specific antibody responses, whereas hCD19Tg mice lacked B-1b cells and adaptive PPS-specific antibody responses. This reciprocal contribution of B-1a and B-1b subsets to innate and acquired immunity reveals an unexpected division of labor within the B-1 compartment that is normally balanced by their coordinated development.

Introduction

B-1 lymphocytes represent a unique B cell population distinguished from conventional B (B-2) cells by their phenotype, anatomical localization, self-renewing capacity, and production of natural antibodies (Berland and Wortis, 2002; Hardy and Hayakawa, 2001). B-1 cells have an $IgM^{hi}IgD^{lo}CD23^{-}B220^{lo}$ phenotype, with Mac-1 expression on peritoneal but not splenic B-1 cells. B-1 cells are subdivided into the B-1a ($CD5^{+}$) and B-1b ($CD5^{-}$) subsets based on cell surface CD5 expression. The origins of B-1 cells and whether B-1a and B-1b cells are derived from the same or distinct progenitor cells are unknown, although B-1a cell development is strongly influenced by B cell antigen receptor (BCR) specificity and strength of signaling. Mice deficient in critical intracellular BCR signaling molecules, including B cell linker protein, Bruton's tyrosine kinase, Vav, phospholipase Cγ2, phosphatidylinositol 3-kinase p85, and protein kinase C, exhibit dramatic reductions in the B-1a cell compartment (Berland and Wortis, 2002; Hardy and Hayakawa, 2001). As a key regulator of B cell signaling, CD19 also plays a prominent role in B-1 cell development. CD19 deficiency impairs B-1a cell development (Engel et al., 1995; Rickert et al., 1995), while CD19 overexpression augments B-1a cell development (Sato et al., 1996). Although BCR and CD19 signaling regulate B-1a cell development, the relative importance of signaling strength to B-1b cell development is unknown.

B-1 cells are envisioned as key players in the early humoral response against pathogens and are thought to be the primary antibody producers in response to T cell-independent type 2 (TI-2) antigens along with marginal zone (MZ) B cells (Martin and Kearney, 2000; Martin et al., 2001). TI-2 antigens are characterized by high molecular weight, repeating epitopes, and slow degradability in vivo. These antigens, such as bacterial capsular polysaccharides, elicit rapid antibody responses by multivalent BCR crosslinking in the absence of major histocompatibility complex class II-restricted T cell help (Mond et al., 1995). Intact responses to TI-2 antigens are critical for the generation of protective immunity to encaspulated extracellular bacteria such as *Streptococcus pneumoniae*, a gram-positive bacteria that is the predominant cause of otitis media, community-acquired pneumonia, septicemia, and meningitis in humans (Wuorimaa and Kayhty, 2002). Preexisting natural antibodies provide innate protection against these types of bacterial infections in naive hosts (Briles et al., 1981; Mi et al., 2000). Immunization-induced antibodies specific for the TI-2 antigen, pneumococcal polysaccharide (PPS), also contribute substantially to protective immune responses against *S. pneumoniae* (Wuorimaa and Kayhty, 2002). As such, the Pneumovax vaccine consists of 23 types of PPS, including pneumococcal polysaccharide type 3 (PPS-3), which elicits specific protection against serotype 3 *S. pneumoniae*, a major cause of invasive pneumococcal disease (Ortqvist, 2001; Wuorimaa and Kayhty, 2002). Impaired PPS responses (Amsbaugh et al., 1972) and inadequate production of natural antibodies important for protection against encapsulated bacteria (Briles et al., 1981) result from defects in B cell signaling pathways, such as those caused by the *xid* mutation. However, the effects of alterations in CD19 expression or CD19-regulated signaling pathways on protective antibody responses to encapsulated bacteria are largely unknown. Furthermore, relatively little is known about the functional contributions of individual B-1a and B-1b subsets despite the proposed importance of B-1 cells in generating protective antibody responses against bacterial antigens.

In this study, the importance of B-1 cell subsets in protection against *S. pneumoniae* infection was examined using CD19-deficient ($CD19^{-/-}$) and CD19-overexpressing (hCD19Tg) mice. B cells from $CD19^{-/-}$ mice are hyporesponsive to transmembrane signals, and $CD19^{-/-}$ mice generate modest immune responses to T cell-dependent (TD) antigens with impaired natural antibody production (Engel et al., 1995; Rickert et al., 1995; Sato et al., 1995, 1996, 1997). By contrast, B cells from hCD19Tg mice are hyperresponsive to mitogens, such as LPS, and hCD19Tg mice generate elevated TD hu-

*Correspondence: thomas.tedder@duke.edu

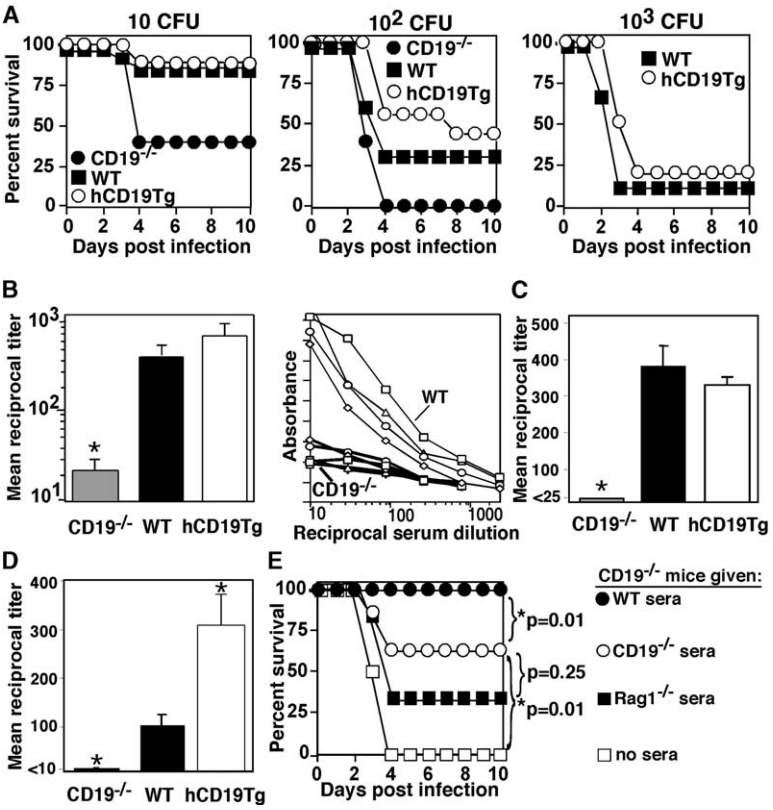

Figure 1. Increased Susceptibility of CD19$^{-/-}$, but Not hCD19Tg, Mice to *S. pneumoniae* Infection Due to Impaired Natural Antibody Production

(A) Survival of CD19$^{-/-}$, wild-type (WT), and hCD19Tg mice following infection with 10, 10^2, or 10^3 cfu *S. pneumoniae*. Each graph represents results from 5–10 mice of each genotype.

(B–D) *S. pneumoniae*-specific natural serum antibody (B), PPS-3-specific IgM (C), and PC-specific IgM (D) titers in CD19$^{-/-}$, WT, and hCD19Tg mice were determined by ELISA using 3-fold serial dilutions, beginning with 1:10 (B and D) or 1:25 (C) dilutions. Values represent mean (±SEM) reciprocal titers from 4–7 mice of each genotype. Individual titers for CD19$^{-/-}$ and WT mouse sera are shown in (B) (right panel). Asterisks represent significant differences between wild-type and other sample means; $p < 0.01$.

(E) WT mouse serum protects CD19$^{-/-}$ mice against infection. CD19$^{-/-}$ mice were given 500 μl of WT (n=21), CD19$^{-/-}$ (n = 24), or Rag1$^{-/-}$ (n = 7) mouse serum i.p. or no serum (n = 8) 2 hr before challenge with ~60 cfu of *S. pneumoniae*. Results represent data pooled from three experiments, with chi-square analysis for group comparisons indicated.

moral immune responses and disrupted tolerance with autoantibody production (Engel et al., 1995; Inaoki et al., 1997; Sato et al., 1995, 1996, 1997; Zhou et al., 1994). The present study demonstrates that B-1b cells are the predominant B-1 cell subset in CD19$^{-/-}$ mice, while B-1a cells develop preferentially in hCD19Tg mice. The reciprocal regulation of B-1a and B-1b development dramatically alters the abilities of CD19$^{-/-}$ and hCD19Tg mice to generate protective humoral responses to *S. pneumoniae*. This shift in B-1 cell subsets revealed that wild-type B-1a cells spontaneously produce natural antibodies important for early protection, while wild-type B-1b cells are the primary source of adaptive antibody responses to PPS during infection and are essential for long-term protection.

Results

CD19 Deficiency Increases Susceptibility to *S. pneumoniae* Infection

The importance of CD19 expression during acute infection was assessed by comparing the susceptibility of CD19$^{-/-}$, wild-type, and hCD19Tg mice to *S. pneumoniae* infection. Mice were infected with 10, 10^2, or 10^3 colony forming units (cfu) of WU2, an encapsulated type 3 strain of *S. pneumoniae*. hCD19Tg and wild-type mice were equally susceptible to *S. pneumoniae*, with 10^2 cfu causing >50% lethality (Figure 1A). By contrast, CD19$^{-/-}$ mice were more susceptible to *S. pneumoniae* infection, with only 10 cfu causing >50% mortality and 10^2 cfu resulting in 100% mortality. Thus, CD19 expression contributes significantly to host defense against acute *S. pneumoniae* infection.

Natural Antibody Production Requires CD19 Expression

To determine whether the enhanced susceptibility of CD19$^{-/-}$ mice to *S. pneumoniae* infection was due to the absence of protective natural antibodies, serum from naive CD19$^{-/-}$, wild-type, and hCD19Tg mice was examined. Serum antibody titers to whole heat-killed *S. pneumoniae* were >20-fold lower in CD19$^{-/-}$ mice compared to wild-type and hCD19Tg mice (Figure 1B). Likewise, CD19$^{-/-}$ mouse sera did not react with PPS-3 or phosphocholine (PC) in contrast with sera from hCD19Tg and wild-type mice (Figures 1C and 1D). In fact, no significant differences were detected in the reactivity of CD19$^{-/-}$ and Rag1$^{-/-}$ mouse sera with whole bacteria or PC (data not shown). However, transferring wild-type mouse serum into CD19$^{-/-}$ mice before challenge with *S. pneumoniae* significantly increased their survival compared to mice given serum from CD19$^{-/-}$ mice (Figure 1E). Moreover, there was no significant difference in survival between CD19$^{-/-}$ mice given CD19$^{-/-}$ mouse serum and Rag1$^{-/-}$ mouse serum. Thus, CD19 deficiency severely impairs natural antibody production, which provides the first level of protection during *S. pneumoniae* infection.

PPS-3 Immunization Protects CD19$^{-/-}$, but Not hCD19Tg, Mice against Infection

The importance of CD19 expression during acquired humoral immune responses to PPS-3 was assessed.

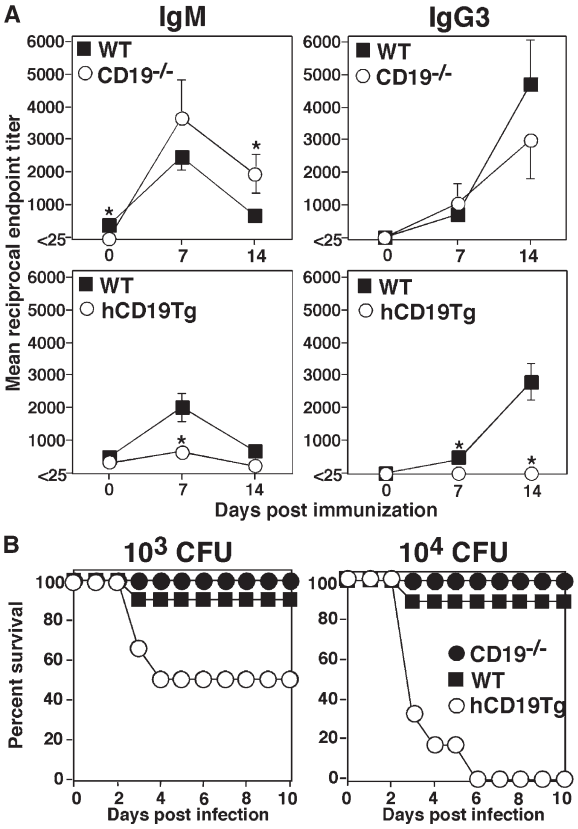

Figure 2. PPS-3 Immunization Elicits Protection in CD19$^{-/-}$, but Not hCD19Tg, Mice during *S. pneumoniae* Challenge

(A) PPS-3-specific antibody responses of CD19$^{-/-}$, wild-type (WT), and hCD19Tg mice. PPS-3-specific titers were determined by ELISA using 3-fold serial dilutions beginning at 1:25. Significant differences between mean (±SEM) titers are indicated by asterisks; *$p < 0.05$ ($n \geq 5$ mice/genotype).

(B) Fourteen days following PPS-3 immunization (as in [A]), 6–8 mice of each genotype were infected with 10^3 or 10^4 cfu of *S. pneumoniae*.

PPS-3-specific IgM was not present in the preimmune sera of CD19$^{-/-}$ mice, but was detectable in sera from hCD19Tg and wild-type mice (Figures 1C and 2A). PPS-3-specific IgG3 was not detected in naive CD19$^{-/-}$, wild-type, or hCD19Tg mice. However, PPS-3 immunization resulted in equal or higher IgM and IgG3 antibody responses in CD19$^{-/-}$ mice than in wild-type mice. By contrast, PPS-3-specific IgM antibody responses were significantly lower in hCD19Tg mice. The absence of measurable PPS-3-specific IgG3 antibodies in hCD19Tg mice after immunization was even more striking. Thus, CD19 expression was not required for normal PPS-3-specific antibody responses following immunization, while CD19 overexpression inhibited PPS-3 antibody responses.

Whether PPS-3 immunization affected susceptibility to *S. pneumoniae* was assessed by challenging CD19$^{-/-}$, wild-type, and hCD19Tg mice with 10^3 or 10^4 cfu of bacteria 14 days following immunization. CD19$^{-/-}$ and wild-type mice were equally protected against these normally lethal doses of *S. pneumoniae* (Figure 2B). By contrast, hCD19Tg mice were significantly more susceptible to infection than wild-type mice ($p < 0.05$, 10^3 cfu challenge; $p < 0.001$, 10^4 cfu challenge). In fact, immunization did not dramatically enhance the survival of hCD19Tg mice (Figure 2B) when compared with naive hCD19Tg mice (Figure 1A; 10^3 cfu dose). Thus, altered CD19 expression clearly influenced protective humoral responses following PPS-3 immunization, but in an unexpected way.

CD19$^{-/-}$ and hCD19Tg Mice Respond Differently to *S. pneumoniae* Immunization

Whether humoral responses to whole bacteria differed from responses to purified PPS-3 was assessed following immunization of CD19$^{-/-}$, wild-type, and hCD19Tg mice with whole heat-killed WU2 bacteria. CD19$^{-/-}$ and wild-type mice generated comparable PPS-3-specific IgM and IgG3 antibody responses (Figure 3A). By contrast, hCD19Tg mice did not produce PPS-3-specific antibodies, but did generate appreciable levels of bacteria-specific antibody (Figures 3A and 3B). *S. pneumoniae*-specific antibody titers were >1:1000 in wild-type mice when assessed by flow cytometry (day 14, Figure 3B). Sera from CD19$^{-/-}$ and hCD19Tg mice also reacted with whole bacteria, but with titers of ~1:100. However, the addition of PPS-3 to the sera inhibited wild-type and CD19$^{-/-}$ serum antibodies from binding to bacteria, but did not diminish the binding of serum antibodies from hCD19Tg mice (Figure 3C). Thus, CD19$^{-/-}$ mice responded optimally to PPS-3, while wild-type mice responded optimally to both PPS-3 and non-PPS-3 antigens. By contrast, PPS-3-specific antibody generation was impaired in hCD19Tg mice, although hCD19Tg mice generated humoral immune responses to other *S. pneumoniae* antigens.

The isotypes of bacteria-specific antibodies produced by CD19$^{-/-}$ and hCD19Tg mice were also clearly different following whole bacteria immunizations. Wild-type mice produced the highest levels of each antibody isotype (Figure 3D), potentially reflecting optimal antibody responses to both TI and TD antigens. By contrast, CD19$^{-/-}$ mice produced substantial IgG3 anti-bacterial antibody responses, but IgG1 responses were not detectable. hCD19Tg mice produced substantial IgG1 anti-bacterial antibody responses, but no detectable IgG3 responses. CD19$^{-/-}$ mice produced higher IgM and IgG2a levels than hCD19Tg mice, while IgG2b levels were similar between CD19$^{-/-}$ and hCD19Tg mice. These results suggest clear differences in the types of bacterial antigens that CD19$^{-/-}$ and hCD19Tg mice respond to.

Antibody responses to PC, a hapten displayed on the cell wall polysaccharide of *S. pneumoniae*, were also assessed following immunizations with whole heat-killed bacteria. Natural anti-PC IgM titers were high in hCD19Tg mice relative to wild-type mice, whereas PC-specific IgM antibodies were absent in CD19$^{-/-}$ mice (Figure 3E). Following bacteria immunizations, wild-type mice produced high IgM and IgG3 anti-PC titers. In comparison, PC-specific IgM titers were reduced 5-fold in hCD19Tg mice and ≥70-fold in CD19$^{-/-}$ mice 7 days post immunization. Moreover, PC-specific IgG3 responses were not detectable in hCD19Tg or CD19$^{-/-}$ mice. Thus, alterations in CD19 expression had distinct effects on humoral immune responses to different bacterial antigens, including PC and PPS-3.

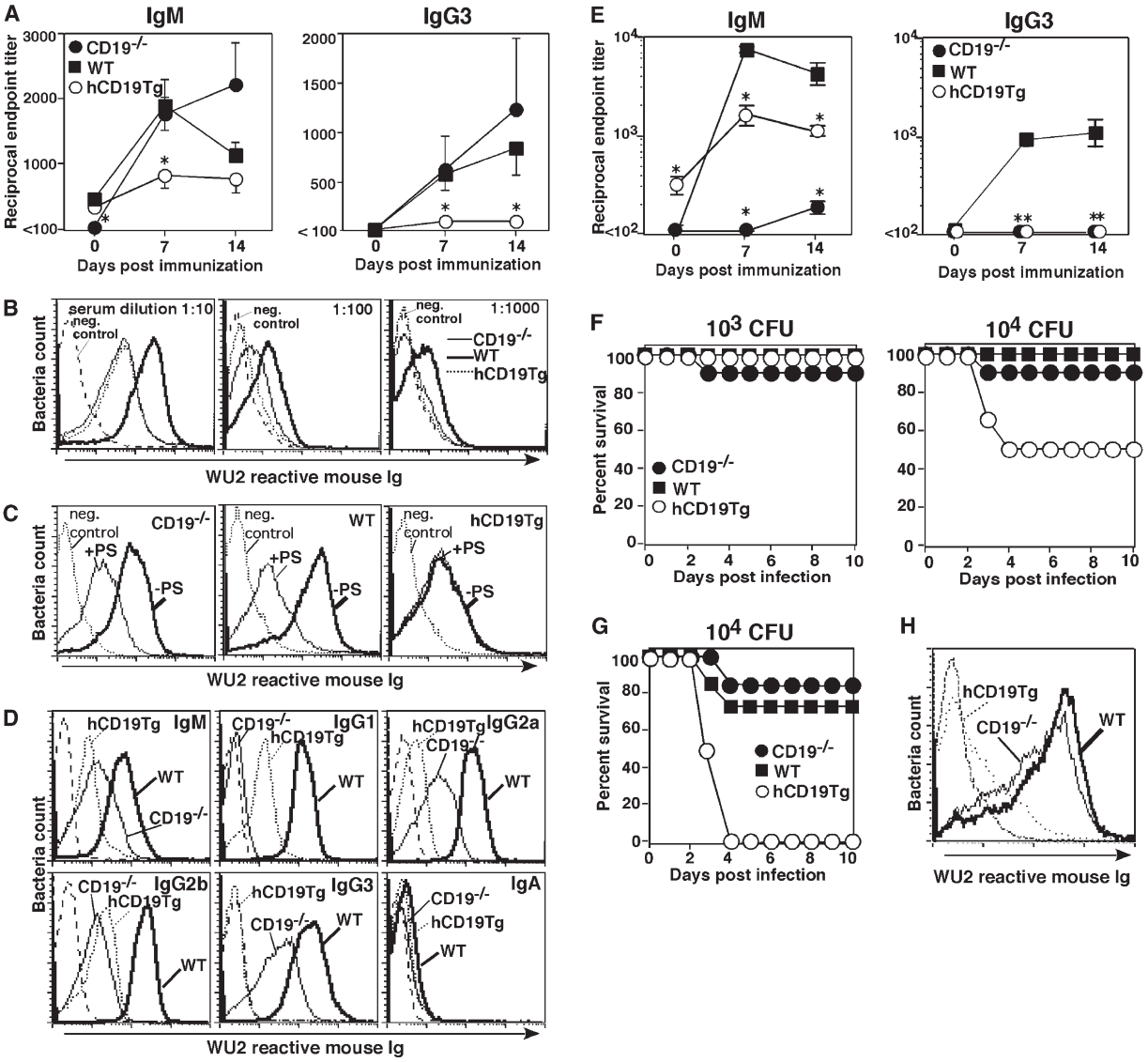

Figure 3. *S. pneumoniae* Immunization Induces Antibody Responses in CD19$^{-/-}$, Wild-Type, and hCD19Tg Mice that Provide Differing Degrees of Protection during Infection

(A) PPS-3-specific antibody responses in mice immunized with heat-killed *S. pneumoniae*. Antibody titers were determined by ELISA using 3-fold serial dilutions beginning at 1:100. Significant differences between mean (±SEM) titers are indicated by asterisks; *$p < 0.05$ ($n \geq 5$ mice per genotype).

(B–D) Serum antibody reactivity with intact bacteria 14 days following immunization with heat-killed *S. pneumoniae* (as in [A]) assessed by indirect immunofluorescence staining with flow cytometry analysis. Pooled serum from eight mice of each genotype was diluted in PBS and incubated with heat-killed bacteria. (B) Reactivity of diluted sera (1:10–1000) from immunized mice. (C) Serum (diluted 1:10) was preincubated with PPS-3 (400 μg/ml final concentration; +PS) or PBS alone (–PS) for 20 min and then assessed for binding to bacteria. (D) Isotypes of *S. pneumoniae*-specific antibodies in wild-type (thick solid line), CD19$^{-/-}$ (thin solid line), and hCD19Tg (dotted line) mouse serum diluted 1:10. Isotype-specific secondary antibodies were used to detect bound antibodies.

(E) PC-specific antibody responses in mice immunized with heat-killed *S. pneumoniae* as determined by ELISA using 3-fold serial dilutions beginning at 1:100. Significant differences between mean (±SEM) titers are indicated by asterisks; *$p < 0.05$ ($n \geq 5$ mice per genotype).

(F) Survival of mice infected 14 days following immunization with *S. pneumoniae* (n = 6 mice/genotype for each challenge dose).

(G–H) Long-term protection of immunized mice against *S. pneumoniae* infection. (G) Survival of mice (6–7 per group) following *S. pneumoniae* challenge 10 weeks after immunization with whole heat-killed bacteria. (H) Bacteria-reactive antibody 10 weeks post immunization with 10^7 heat-killed WU2 assessed by flow cytometry. Staining with secondary antibody alone is indicated by dashed lines.

Immunization Provides Long-Lasting Protection in CD19$^{-/-}$ Mice, but Not in hCD19Tg Mice

To determine if whole bacteria immunization induced protective antibodies, CD19$^{-/-}$, wild-type, and hCD19Tg mice were immunized with heat-killed bacteria. Fourteen days later, the mice were challenged with 10^3 or 10^4 cfu of bacteria, doses that resulted in 100% mortality in naive wild-type mice (data not shown). Prior immunization with whole bacteria protected CD19$^{-/-}$ and wild-type mice from bacterial challenge (Figure 3F).

Table 1. B Lymphocyte Subsets in CD19$^{-/-}$ and hCD19Tg Mice

	% of B220$^+$ Lymphocytes[a]			Lymphocyte Numbers (× 10^{-5})[b]			% of Total Lymphocytes		
Phenotype[c]	CD19$^{-/-}$	Wild-Type	hCD19Tg	CD19$^{-/-}$	Wild-Type	hCD19Tg	CD19$^{-/-}$	Wild-Type	hCD19Tg
Peritoneal Cavity									
B-1a	2 ± 1*	14 ± 1	70 ± 3*	0.07 ± .02*	1.6 ± 0.2	5.6 ± 0.6*	1 ± 1*	10 ± 1	28 ± 2*
B-1b	58 ± 4*	40 ± 2	4 ± 1*	1.2 ± 0.2*	4.3 ± 0.6	0.3 ± 0.1*	27 ± 2	27 ± 1	2 ± 1*
B-2	39 ± 4	46 ± 4	25 ± 2*	1.0 ± 0.3*	4.3 ± 0.6	1.6 ± 0.2*	19 ± 2*	32 ± 3	10 ± 1*
B220$^+$	100	100	100	2.3 ± 0.5*	10 ± 0.1	8 ± 0.9	47 ± 2*	66 ± 2	40 ± 2*
Lymphocytes				4.7 ± 1.0*	15 ± 0.2	20 ± 0.2			
Spleen									
B-1a	4 ± 1*	8 ± 1	24 ± 3*	8 ± 2*	36 ± 2	31 ± 8	2.1 ± 0.1*	4.2 ± 0.4	7.0 ± 0.5*
B-2	80 ± 2	69 ± 1	40 ± 5*	165 ± 46*	326 ± 29	51 ± 12*	38 ± 3	39 ± 1	14 ± 1*
MZ	6 ± 1*	13 ± 2	12 ± 1	12 ± 2*	64 ± 14	16 ± 6*	3.2 ± 0.3*	7.3 ± 1.3	3.5 ± 0.5*
B220$^+$	100	100	100	206 ± 56*	472 ± 42	133 ± 38*	53 ± 4	55 ± 3	30 ± 2*
Lymphocytes				627± 141*	1,220 ± 44	713 ± 19*			

*The percentage or number of cells was significantly different from that of wild type mice, *$p < 0.05$.
[a] Values represent the mean frequency (±SEM) of lymphocytes (based on side and forward angle light scatter) expressing the indicated surface markers as determined by immunofluorescence staining with flow cytometry analysis. Results were from 3–12 mice of each genotype.
[b] Mean B cell numbers (±SEM) were calculated based on the total number of cells harvested from spleen or the peritoneal cavity.
[c] Cells were identified as follows: splenic B-2 cells, B220^{hi}CD23$^+$CD21^{int}; splenic B-1a cells, B220$^+$CD5$^+$; MZ B cells, B220$^+$CD1d^{hi}CD21^{hi}; peritoneal B-2, B220$^+$CD11b$^-$CD5$^-$; peritoneal B-1a, B220$^+$CD11b$^+$CD5$^+$; and peritoneal B-1b cells, B220$^+$CD11b$^+$CD5$^-$.

However, only half of hCD19Tg mice were protected from infection at a 10^4 cfu challenge dose. Thus, whole bacteria immunizations induced lower protective antibody responses in hCD19Tg mice than in CD19$^{-/-}$ and wild-type mice.

The duration of protective antibody responses was assessed using mice that had been immunized once with 10^7 heat-killed bacteria and had survived lethal challenge as shown in Figure 3F. These mice were rechallenged with 10^4 cfu 10 weeks after immunization. Both CD19$^{-/-}$ and wild-type mice were equally protected during reinfection (Figure 3G). However, all hCD19Tg mice succumbed to this secondary infection by day 4 post challenge ($p = 0.04$, χ^2 analysis; hCD19Tg versus wild-type survival). The susceptibility of hCD19Tg mice to reinfection correlated with their dramatic loss of serum antibodies reactive with whole bacteria, while wild-type and CD19$^{-/-}$ mice maintained antibodies reactive with bacteria for at least 10 weeks post immunization (Figure 3H). Thus, protective humoral immune responses generated in CD19$^{-/-}$ and hCD19Tg mice were qualitatively and quantitatively distinct.

CD19$^{-/-}$ and hCD19Tg Mice Have Distinct B-1 Cell Subsets

Both CD19$^{-/-}$ and hCD19Tg mice have significantly reduced numbers of splenic B cells compared to wild-type mice (Table 1), particularly B-2 cells as described (Engel et al., 1995; Sato et al., 1995, 1997). CD19 deficiency also impairs B-1a cell development in the spleen, while CD19 overexpression favors B-1a cell development (Engel et al., 1995; Rickert et al., 1995; Sato et al., 1996). As a result, total spleen B-1a (CD5$^+$B220$^+$) cell numbers were 78% lower in CD19$^{-/-}$ mice, while B-1a cells were present at normal numbers in hCD19Tg mice despite reduced numbers of B-2 cells (Table 1). The frequency and number of peritoneal cavity B-2 (CD5$^-$CD11b$^-$B220$^+$) cells were also significantly decreased in CD19$^{-/-}$ mice and hCD19Tg mice compared to wild-type mice (Table 1).

The frequencies of peritoneal B-1a and B-1b cells were clearly different between CD19$^{-/-}$, wild-type, and hCD19Tg mice when CD5 expression was used to differentiate peritoneal B-1a (CD5$^+$CD11b$^+$) and B-1b (CD5$^-$CD11b$^+$) cells. Although the peritoneal CD11b$^+$ B cell population exhibited an IgM^{hi} phenotype in all mice, the vast majority of CD11b$^+$B220$^+$ cells were CD5$^-$ in CD19$^{-/-}$ mice, while the majority of B-1 cells in hCD19Tg mice coexpressed CD5 (Table 1; Figure 4A). In wild-type mice, ~30% of CD11b$^+$B220$^+$ cells coexpressed CD5. In CD19$^{-/-}$ mice, the frequency of B-1b cells among total peritoneal B220$^+$ cells was significantly higher than in wild-type mice (58% ± 4% versus 40% ± 2%; Table 1). By contrast, the number and frequency of B-1a cells was 3- to 5-fold higher in hCD19Tg mice than wild-type mice, whereas the number and frequency of B-1b cells was ≥90% lower (Table 1). Moreover, the few CD11b$^+$B220$^+$ cells that appeared CD5$^-$ in hCD19Tg mice actually expressed CD5 at densities (mean fluorescence intensity values) that were ~2-fold higher ($p < 0.05$) than CD5$^-$CD11b$^+$B220$^+$ cells from wild-type or CD19$^{-/-}$ mice (data not shown). Thus, the majority of peritoneal B-1 cells in hCD19Tg mice exhibit a B-1a phenotype, while the majority of B-1 cells in CD19$^{-/-}$ mice exhibit a B-1b phenotype.

MZ B Cell Development in CD19$^{-/-}$ and hCD19Tg Mice

In CD19$^{-/-}$ mice, MZ B cell numbers and frequencies were significantly reduced (81% and 54%, respectively; Table 1, Figure 4B) as described for different lines of CD19$^{-/-}$ mice (Makowska et al., 1999; Wang et al., 2002). Although the frequency of MZ B cells among B220$^+$ cells (12%–13%) was similar between hCD19Tg and wild-type mice (Figure 4B), total spleen B cell numbers were significantly reduced in hCD19Tg mice (Table 1). As a result, MZ B cell numbers were also significantly lower (~75% reduced) in hCD19Tg mice compared to wild-type mice (Table 1). Immunohistochemical analysis of spleen tissue sections from CD19$^{-/-}$ and hCD19Tg

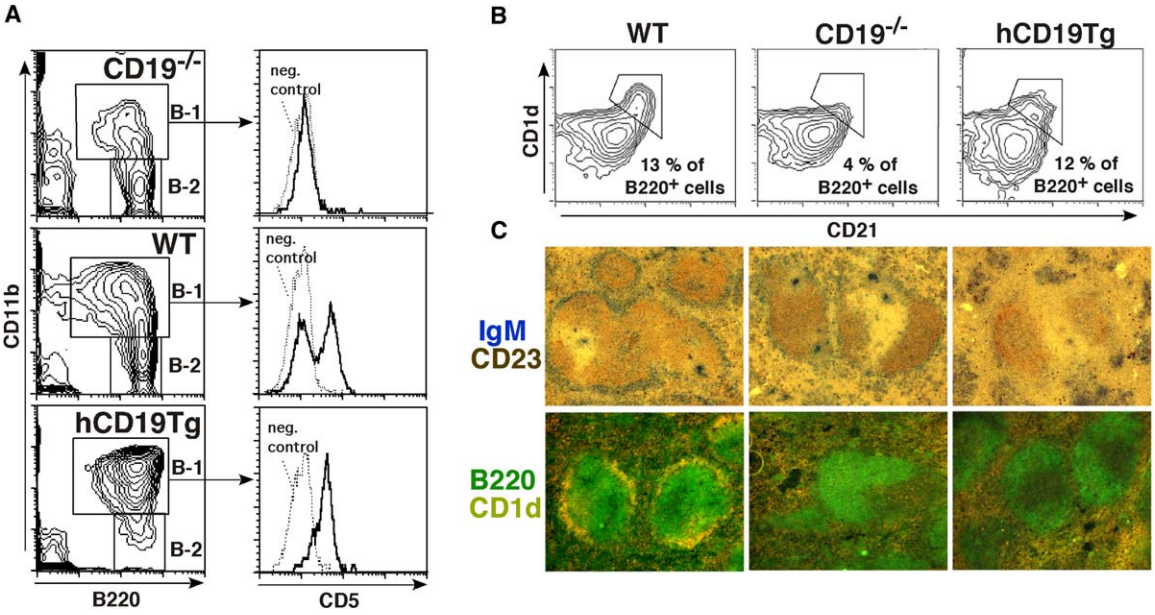

Figure 4. B-1 and MZ B Cell Subsets in CD19$^{-/-}$, Wild-Type, and hCD19Tg Mice

(A) Three-color staining of peritoneal B cells for B220, CD11b, and CD5 expression with flow cytometry analysis. B-1 (B220^{+}CD11b^{+}) and B-2 (B220^{+}CD11b^{-}) lymphocytes are indicated (left column) with histograms showing CD5 expression by peritoneal B-1 (B220^{+}CD11b^{+}-gated) cells (right column). Isotype-matched control antibody staining is indicated by a dotted line.

(B) Frequencies of CD21^{hi}CD1d^{hi} MZ B cells among the B220^{+}-gated spleen cell population.

(C) Immunohistochemical analysis of spleen sections. Upper sections were stained for CD23 (brown) and IgM (blue). Lower sections were stained for CD1d (red) and B220 (green), with CD1d^{hi}B220^{+} cells characterized by yellow fluorescence in overlaid digital microscopy images. Original magnification: 200×. All results represent those obtained with $\geq$3 mice of each genotype.

mice confirmed these results. In wild-type mice, an IgM^{bright} population of cells surrounded CD23^{bright} follicles, or a distinct B220^{+}CD1d^{bright} rim of MZ B cells surrounded follicles (Figure 4C). However, only a thin rim of CD23$^{dull/-}$IgM^{bright} cells was identified in spleen sections of CD19$^{-/-}$ mice, while a region of B220^{+} CD1d^{bright} MZ cells was difficult to discern (Figure 4C). An organized MZ-like region of CD23$^{dull/-}$IgM^{bright} cells or B220^{+}CD1d^{bright} staining was not identifiable in hCD19Tg mice, consistent with their significant reduction in MZ B cell numbers (Table 1) and overall reduced IgM expression (Engel et al., 1995; Rickert et al., 1995; Sato et al., 1995, 1996, 1997). In addition, the MZs of CD19$^{-/-}$ and hCD19Tg mice were insufficient to capture complement-tagged antigens entering the spleen via the blood unlike wild-type mice, as assessed using C3dg-SA-PE tetramer complexes (data not shown) (Haas et al., 2002). Thus, both CD19 deficiency and CD19 overexpression impair splenic MZ B cell development.

B-1a Cells Produce Natural Antibody Reactive with *S. pneumoniae*

To determine if B-1a cell deficiency in CD19$^{-/-}$ mice explained their inability to generate natural serum antibody reactive with *S. pneumoniae* (Figures 1B–1D), peritoneal and splenic B-1a cells were transferred into Rag1$^{-/-}$ mice and assessed for their ability to spontaneously produce PPS-3-reactive antibody. Since hCD19Tg mice exhibit an expanded B-1a cell population, the peritoneal cavity and spleens of these mice were used as a source of B-1a (CD5^{+}CD11b^{+}B220^{+}) cells. B-1a cells represented ~34% of the peritoneal cavity lymphocytes used for adoptive transfer (Figure 5A), whereas CD5^{-}CD11b^{-}B220^{+} cells comprised only ~1% of lymphocytes (data not shown). Transfer of peritoneal hCD19Tg B cells into Rag1$^{-/-}$ mice resulted in the generation of serum immunoglobulin, including PPS-3-reactive natural antibodies (Figure 5B). Likewise, transfer of purified splenic B-1a cells into Rag1$^{-/-}$ mice resulted in the generation of serum immunoglobulin and PPS-3-reactive natural antibodies (Figure 5B). Comparable peritoneal B cell numbers were recovered from mice that had received hCD19Tg peritoneal cells ($1.5 \pm 0.5 \times 10^5$) or spleen B-1a cells ($1.5 \pm 0.9 \times 10^5$). Furthermore, recovered peritoneal (CD19^{+}) B cells coexpressed CD5 and CD11b, indicating their B-1a phenotype (Figure 5C). However, Rag1$^{-/-}$ mice that had received B-1a cells from hCD19Tg mice did not significantly augment PPS-3 reactive antibody levels following immunization with PPS-3 (Figure 5D). Thus, B-1a cells are primarily a source of natural antibodies that may contribute to protection against *S. pneumoniae* infection.

B-1b Cells from CD19$^{-/-}$ Mice Generate Adaptive Antibody Responses to PPS-3

To determine if differences in B-1 subsets explained the dramatic differences in PPS-3 antibody responses between CD19$^{-/-}$ and hCD19Tg mice, peritoneal B-1b (CD5^{-}CD11b^{+}B220^{+}) and B-2 (CD5^{-}CD11b^{-}B220^{+}) cells

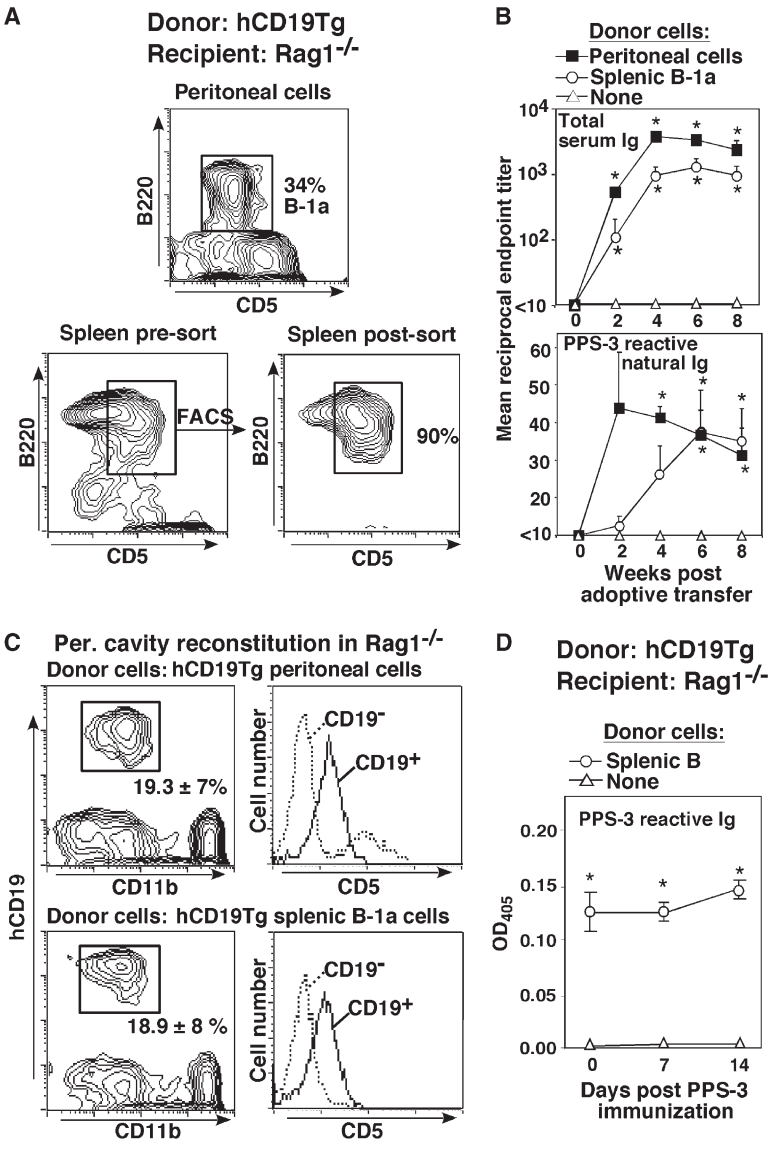

Figure 5. Peritoneal and Splenic B-1a Cells Transferred into Rag1$^{-/-}$ Mice Produce PPS-3-Reactive Natural Antibody

(A) Peritoneal cavity lymphocytes (5 × 10^6) or FACS-purified splenic B-1a cells (CD5$^+$B220$^+$; 1 × 10^6) from hCD19Tg mice were transferred i.p. into Rag1$^{-/-}$ mice (four mice/group).

(B) Total serum immunoglobulin (Ig; upper graph) and PPS-3-reactive natural antibodies (lower graph) in sera of Rag1$^{-/-}$ mice following adoptive transfers. Values represent mean (±SEM) antibody titers from 3–4 mice/group.

(C) B cell reconstitution in Rag1$^{-/-}$ mice 8 weeks following adoptive transfer. Peritoneal cavity lymphocytes harvested from Rag1$^{-/-}$ recipient mice were stained with antibodies against mouse CD11b, CD5, and human CD19 (hCD19) and analyzed by flow cytometry. Percentages indicate mean (±SEM) hCD19$^+$CD11b$^+$ cell frequencies for each recipient group. Representative CD5 expression levels are shown for the hCD19$^+$ and hCD19$^-$ populations.

(D) PPS-3-specific IgM in Rag1$^{-/-}$ mice following adoptive transfer of hCD19Tg spleen B cells and PPS-3 immunization. Ten weeks following adoptive transfer, Rag1$^{-/-}$ mice were immunized i.p. with 0.5 μg PPS-3. PPS-3-specific IgM levels were measured by ELISA using serum samples diluted 1:25. Differences between mean (±SEM) titers or OD values of recipient and nonrecipient Rag1$^{-/-}$ mice were significant; *p < 0.05 (n = 3–4 mice/group).

from CD19$^{-/-}$ mice were purified (Figure 6A) and adoptively transferred into hCD19Tg mice. Spleen and lymph node B cells from CD19$^{-/-}$ mice were also transferred into hCD19Tg mice. Three weeks after cell transfer, the hCD19Tg mice were immunized with PPS-3. IgM antibody responses to PPS-3 were present in mice that had received peritoneal B-1b cells but not in mice that had received peritoneal B-2 cells or spleen and lymph node B cells (Figure 6B). Thus, peritoneal B-1b cells from CD19$^{-/-}$ mice restored IgM responses to PPS-3 in hCD19Tg mice.

B-1b Cells from Wild-Type Mice Generate Adaptive Antibody Responses to PPS-3

Peritoneal B-1b cells from wild-type mice were also responsible for antibody responses to PPS-3. Spleen B cells or peritoneal B-1a (CD5$^+$CD11b$^+$B220$^+$) and B-1b (CD5$^-$CD11b$^+$B220$^+$) cells were purified from wild-type mice (Figure 6C) and transferred into Rag1$^{-/-}$ mice. Four weeks after cell transfer, the mice were immunized with PPS-3. Rag1$^{-/-}$ mice receiving B-1b cells generated anti-PPS-3 IgM responses that were significantly higher than mice that had received B-1a cells, spleen B cells, or no cells (Figure 6D). Importantly, analysis of peritoneal B cells in Rag1$^{-/-}$ mice 8 weeks post transfer demonstrated that ≥93% of peritoneal IgM$^+$ cells from B-1a, B-1b, and spleen B cell recipients expressed CD11b, indicating that B-1 cells had primarily survived and/or expanded within the peritoneal cavity following adoptive transfer. The majority of IgM$^+$ cells in B-1b recipients were CD5$^-$ (80% ± 1%), while the majority of IgM$^+$ cells in B-1a recipients were CD5$^+$ (60% ± 6%). There was no significant difference in IgM$^+$ cell numbers recovered from the peritoneum of B-1b recipients (4.2 ± 1.4 × 10^4) or B-1a recipients (2.3 ± 0.3 × 10^4), while there were 10-fold fewer peritoneal IgM$^+$ cells in mice that had received spleen B cells (4 ± 1 × 10^3). Significant numbers of IgM$^+$ cells were also recovered

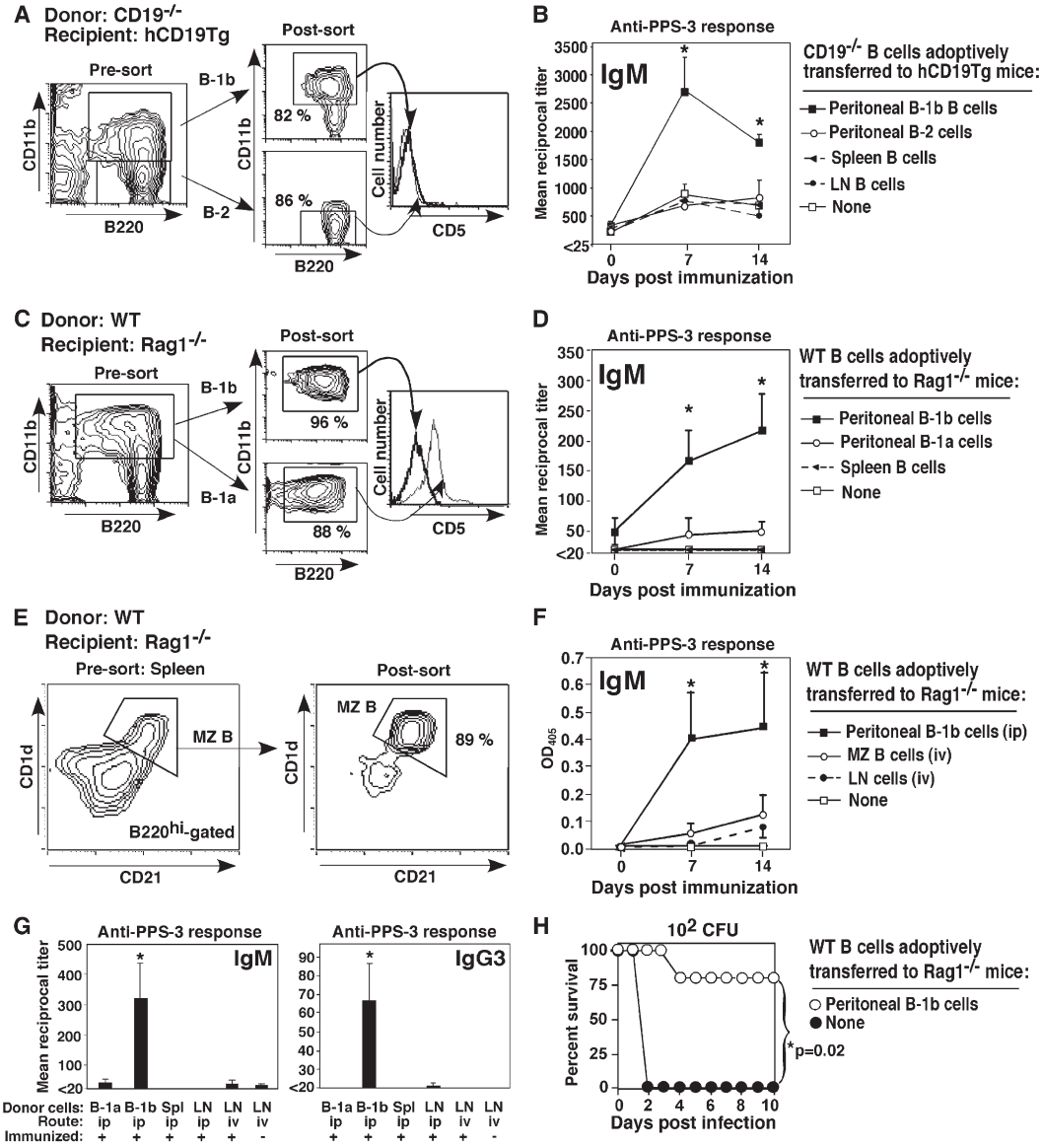

Figure 6. B-1b Cells Generate PPS-3-Specific Antibodies and Provide Protection during *S. pneumoniae* Infection

(A–B) Reconstituting hCD19Tg mice with peritoneal B-1b cells from CD19$^{-/-}$ mice initiates responsiveness to PPS-3. (A) Peritoneal B-1b ($CD5^-CD11b^+B220^+$) or B-2 ($CD5^-CD11b^-B220^+$) cells from CD19$^{-/-}$ mice were isolated by FACS with the frequency of purified cells and CD5 expression indicated. (B) Purified peritoneal B cells or enriched spleen and lymph node B cells from CD19$^{-/-}$ mice were transferred i.p. into hCD19Tg mice (10^5 cells/mouse). Mice were immunized with PPS-3 3 weeks later with PPS-3-specific antibody titers determined by ELISA using 3-fold serial dilutions beginning at 1:25. Values represent mean (±SEM) titers obtained using $\geq$4 mice/group in two independent adoptive transfer-immunization experiments.

(C–G) Reconstituting Rag1$^{-/-}$ mice with peritoneal B-1b cells from wild-type (WT) mice initiates responsiveness to PPS-3. (C) Peritoneal B-1a ($CD5^+CD11b^+B220^+$) or B-1b ($CD5^-CD11b^+B220^+$) cells were purified from WT mice as described in (A). (D) Purified peritoneal B cells or spleen B cells from WT mice were transferred into Rag1$^{-/-}$ mice by i.p. injection (10^5 cells/mouse). Mice were immunized with PPS-3 4 weeks later, with PPS-3-specific antibody titers determined by ELISA using 3-fold serial dilutions beginning at 1:20. Results represent two independent adoptive transfer experiments ($CD5^-CD11b^+B220^+$, n = 6; $CD5^+CD11b^+B220^+$, n = 5; $Thy1.2^-$ spleen cells, n = 3; and Rag1$^{-/-}$ no cell control, n = 3). (E–F) B-1b cells generate larger PPS-3-specific antibody responses than other B cell subsets. (E) MZ B cells ($B220^{hi}CD21^{hi}CD1d^{hi}$) were purified by FACS with the frequency of purified cells indicated. (F) MZ B (E) and unfractionated lymph node cells from WT mice were transferred i.v. into Rag1$^{-/-}$ mice (10^5 B cells/mouse). Purified peritoneal B-1b cells were transferred into Rag1$^{-/-}$ mice by i.p. injection (10^5 B cells/mouse). Mice were immunized with 0.5 μg PPS-3 2 days later, with PPS-3-specific antibody levels determined by ELISA using serum samples diluted 1:25. (B, D, and F) Differences between mean (±SEM) titers or OD values of recipient and nonrecipient mice were significant; *p < 0.05 (n $\geq$ 3 mice/group). (G) Purified WT peritoneal B-1a cells, B-1b cells, or unfractionated spleen or LN cells were transferred i.p. or i.v. into Rag-1$^{-/-}$ mice (4×10^5 B cells/mouse; $\geq$3 mice/group) as indicated. Mice were immunized with 0.5 μg PPS-3 3 days later, with PPS-3-specific IgM (d7) and IgG3 (d14) antibody levels measured by ELISA using serum samples diluted 1:20. Differences between mean (±SEM) titers of immunized mice were significantly different from nonimmunized mice receiving lymph node cells; *p < 0.05.

(H) B-1b cells provide protection during *S. pneumoniae* infection. Rag1$^{-/-}$ mice were given 4×10^5 purified WT peritoneal B-1b cells i.p (n = 5) or no cells (n = 7). Mice were immunized with 0.5 μg PPS-3 3 days later. Mice were infected with 10^2 cfu *S. pneumoniae* 14 days postimmunization. *Chi-square analysis indicates survival was significantly different between groups.

from the spleens of mice that had received peritoneal B-1b ($13 \pm 4 \times 10^4$), B-1a ($7 \pm 1 \times 10^4$), and spleen ($4 \pm 1 \times 10^4$) B cells, but they were $CD11b^-$. Thus, peritoneal B-1a and B-1b cells from wild-type mice reconstituted $Rag1^{-/-}$ mice to comparable degrees. However, PPS-3-specific IgM responses were only found in mice reconstituted with B-1b cells.

The relative roles for peritoneal B-1a, B-1b, MZ, spleen, and lymph node B cells in PPS-3 responses was also assessed using wild-type B cells in short-term adoptive transfer experiments. Purified peritoneal B-1b cells (10^5) were transferred i.p. into $Rag1^{-/-}$ mice. $B220^{hi}CD1d^{hi}CD21^{hi}$ MZ B cells (10^5) or lymph node lymphocytes containing 10^5 B cells were transferred i.v. into $Rag1^{-/-}$ mice (Figure 6E). Two days later, the mice were immunized with PPS-3. B-1b cell recipients produced rapid and robust anti-PPS-3 antibody responses, whereas PPS-3-specific responses were insignificant in MZ and lymph node B cell recipients (Figure 6F). The absence of an antibody response was not due to an absence of B cells since mice receiving MZ B cells contained $2.7 \pm 1.5 \times 10^4$ IgM^+ cells, while mice receiving lymph node cells had $2.2 \pm 1.3 \times 10^4$ IgM^+ spleen B cells 21 days after transfer. To further verify these results, similar experiments were carried out using 4-fold higher numbers of B-1a, B-1b, spleen, or lymph node cells given i.p. and/or i.v. Significant IgM and IgG3 PPS-3-specific antibody responses were rapidly generated in $Rag1^{-/-}$ mice reconstituted with B-1b cells, but not in $Rag1^{-/-}$ mice reconstituted with peritoneal B-1a, spleen, or lymph node cells (Figure 6G). Intravenous transfers of 10-fold higher numbers of lymph node B cells (10^6/mouse) into $Rag1^{-/-}$ mice increased PPS-specific antibody levels after immunization, but $4 \pm 2 \times 10^3$ $CD5^-CD11b^+IgM^{hi}$ cells were found in the peritoneal cavities, but not spleens, of these $Rag1^{-/-}$ mice (data not shown). Similarly, i.p. transfers of higher numbers of spleen B cells depleted of $CD21^{hi}CD1d^{hi}$ MZ B cells (5×10^6/mouse) resulted in significant PPS-specific antibody levels following immunization at 5 weeks post cell transfer, but $6 \pm 1 \times 10^4$ $CD5^-CD11b^+IgM^{hi}$ B cells were found in the peritoneal cavities, but not spleens, of these $Rag1^{-/-}$ mice (data not shown). Thus, B-1b cells or B-1b cell precursors in lymph nodes and spleen may also contribute to PPS-specific antibody responses. Although these experiments do not eliminate a role for B-2 cells in PPS-3 antibody responses, they demonstrate that B-1b cells are primarily responsible for the rapid and robust PPS-3 responses necessary for protection against *S. pneumoniae* infection.

Wild-Type B-1b Cells Provide Protection during *S. pneumoniae* Infection

To determine if B-1b cells provide protection during *S. pneumoniae* infection, $Rag1^{-/-}$ mice were reconstituted with wild-type B-1b cells and immunized with PPS-3. Two weeks later, the mice were challenged with a lethal dose (10^2 cfu) of *S. pneumoniae*. Remarkably, $Rag1^{-/-}$ mice reconstituted with B-1b cells were significantly protected from infection compared to nonreconstituted mice (Figure 6H). Thus, B-1b cells can provide significant protection during *S. pneumoniae* infection.

Discussion

This study reveals an unanticipated equilibrium between B-1a and B-1b cell development in wild-type mice that balances innate and adaptive humoral immune responses during *S. pneumoniae* infection. Specifically, B-1a cells from wild-type or hCD19Tg mice were important for natural antibody production, while B-1b cells from wild-type or $CD19^{-/-}$ mice functioned independently to regulate protective anti-PPS responses to *S. pneumoniae*. In addition, the B-1b subset was required for generating long-lasting protective responses to *S. pneumoniae*, as recently shown for *Borrelia hermsii* immunity (Alugupalli et al., 2004). While this division of labor was unanticipated, equally unexpected was the finding that reciprocal alterations in CD19 expression differentially regulated the balance between B-1a and B-1b cell development and thereby the generation of innate and adaptive antibody responses required for protection against *S. pneumoniae*. CD19 deficiency impaired B-1a development and the production of protective natural antibody, while CD19 overexpression impaired B-1b development and adaptive responses to PPS-3. Although there is evidence to suggest that CD19 signaling activity is differentially regulated in B-1 subsets as compared to conventional B cells (Krop et al., 1996; Sen et al., 2002), our studies do not address a biochemical role for CD19 in the B cell activation pathways elicited during responses to bacterial infection or reveal how CD19 balances the development or homeostasis of the B-1a versus B-1b cell compartments. However, they do demonstrate that alterations in this single cell surface molecule have dramatic effects on natural and acquired antibody production by differentially regulating the balance between B-1a and B-1b cell development.

B-1a cells were primarily responsible for natural antibody production, which was conferred with adoptive transfer of these cells. B-1 cells in hCD19Tg mice were primarily B-1a cells, and these mice had normal to augmented levels of natural antibodies and exhibited normal resistance to acute *S. pneumoniae* infection. However, hCD19Tg mice did not generate PPS-3-specific antibodies in response to PPS-3 or whole bacteria immunizations. Furthermore, antibody responses to whole bacteria were restricted to non-IgG3 isotypes and only provided short-lived humoral immunity that left hCD19Tg mice susceptible to infection. By contrast, B-1b cells were responsible for acquired antibody responses to PPS-3, which were conferred with the adoptive transfer of these cells. Because B-1 cells in $CD19^{-/-}$ mice were primarily, if not exclusively, B-1b cells, these mice were deficient in natural antibodies and were thereby more susceptible to *S. pneumoniae* infection in the absence of immunization or previous exposure. However, $CD19^{-/-}$ mice generated robust IgM and IgG3 antibody responses to PPS-3 and whole bacteria immunizations, which rendered them resistant to infection and led to long-lived humoral immunity. Wild-type B-1b cells also significantly protected PPS-3-immunized $Rag1^{-/-}$ mice during *S. pneumoniae* infection. The importance of having both B-1a and B-1b subsets is exemplified by the results from wild-type mice, which generate both natural and acquired PPS-3

antibody responses and are thus afforded the greatest level of protection against infection. Importantly, in naive hosts, B-1a cell-derived natural antibodies are particularly essential for establishing a basal level of protection during an infection. In the absence of natural antibodies, the host may not be initially protected from death such that B-1b cells may not have the opportunity to respond to an infection. Thus, B-1a and B-1b cell compartments both have critical yet distinct roles in generating protective immunity to *S. pneumoniae.*

The relationship between B cells that produce natural antibodies and those which produce antibody upon pathogen encounter has not been entirely clear (Baumgarth et al., 1999; Kenny et al., 1983; Masmoudi et al., 1990). Likewise, the relationship between B-1a and B-1b cell development is unclear (Berland and Wortis, 2002; Hardy and Hayakawa, 2001; Herzenberg, 2000). However, the current studies reveal distinct and nonredundant functional roles for B-1a and B-1b subsets during innate and adaptive immune responses to *S. pneumoniae* infection, respectively. These findings demonstrate that the B-1b cell subset that is induced to respond to PPS may be fundamentally different from the B-1a cell subset that produces natural antibodies reactive with PPS. Moreover, these two subsets may require different signals or signaling thresholds for their development, activation, and/or differentiation into antibody-producing cells. In agreement with these proposals, others have suggested that B cells which produce antigen-reactive natural antibody before antigen encounter are distinct from the B cells that participate in acquired immune responses to antigen (Baumgarth et al., 1999). In contrast to our findings, a recent study demonstrated a correlation between the absence of B-1a cells and poor responsiveness to PPS (Wardemann et al., 2002). Moreover, this study reported that fetal liver, but not adult bone marrow, cells reconstituted PPS responses in immunodeficient mice. Although the antibody response was interpreted to be due to fetal liver-derived B-1a cells, it is entirely possible that fetal B-1b cells produced the PPS-specific antibody. Indeed, the current study and other studies indicate that the B-1b cell subset is important for antibody responses to PPS and other clinically relevant TI antigens (Alugupalli et al., 2004; Ohdan et al., 2000).

B-1 and MZ B cells are proposed to provide protection during early responses against TI blood-borne particulate antigens through natural antibody production and antibody responses to TI-2 antigens (Martin and Kearney, 2000; Martin et al., 2001). However, MZ B cells did not produce anti-PPS-3 responses in the adoptive transfer experiments performed in this study. In addition, treatments that preferentially deplete MZ B cells, but not B-1b cells, have no effect on PPS-3-specific antibody responses in wild-type mice (K.M.H. and T.F.T., unpublished data). Nonetheless, MZ B and B-1a cells may be important for responses against other TI bacterial antigens, such as PC. In support of this, hCD19Tg mice generated PC-specific natural antibodies as well as an IgM anti-PC response following whole bacteria immunization, while CD19$^{-/-}$ mice did not. These findings highlight a clear and fascinating difference between the factors that are required for anti-PPS responses compared to anti-PC responses, both of which contribute to protection during infection (Amsbaugh et al., 1972; Briles et al., 1981). Therefore, B-1a, B-1b, and MZ B cell subsets may play distinct roles in antibody responses to different TI bacterial antigens.

In summary, the production of acquired antibody responses against capsular polysaccharides by B-1b cells and natural antibody by B-1a cells links innate and adaptive humoral immune responses necessary for complete protection against *S. pneumoniae*. Since alterations in CD19 expression affected the balance between B-1a cell-generated natural antibody production and B-1b cell-generated adaptive antibody responses in such a significant way, it is likely that alterations in additional signaling pathways will have a similar potent impact. Altered signaling pathways, such as those resulting from CD19 overexpression, may also regulate PPS-3 antibody responses by directly regulating B cell activation or skewing the B cell repertoire, thereby affecting the ability of B cells to respond to PPS-3 or other bacterial antigens. However, hCD19Tg mice produced natural antibodies reactive with PPS-3, yet were unable to produce PPS-3-specific antibody following immunization. Thus, PPS-3-reactive B cells exist within the hCD19Tg repertoire, but they were not expanded following bacterial challenge, presumably due to the absence of responding B-1b cells as proposed in this study. Indeed, alterations in B-1 subset development or function due to deviations in B cell signaling pathways or the other factors cited above may explain the heterogeneous responses of outbred populations to vaccines and their susceptibilities to infection. For example, the skewed predominance of the B-1a cell subset early during development (Bhat et al., 1992; Herzenberg, 2000) as well as the predominance of CD5^{+} B cells observed in patients with selective anti-polysaccharide deficiency (Antall et al., 1999) may in part explain the impaired anti-polysaccharide responses and increased incidence of encapsulated bacterial infections in these patients (Ortqvist, 2001). The global burden of pneumococcal disease creates an urgent need to delineate the factors that influence susceptibility to infection and vaccine efficacy. The current study provides an important example of necessary factors that must be considered in eliciting effective antibody responses to encapsulated bacteria such as *S. pneumoniae*. As such, further elucidation of B-1b subset development and function may provide novel opportunities to improve vaccine strategies.

Experimental Procedures

Mice

CD19$^{-/-}$ and hCD19Tg (h19-1 line) mice were as described (Engel et al., 1995; Sato et al., 1996, 1997; Zhou et al., 1994). CD19$^{-/-}$ and hCD19Tg mice were backcrossed with C57BL/6 mice for 14 and 7 generations, respectively. Wild-type C57BL/6 mice and Rag1$^{-/-}$ (B6.129S7-*Rag1^{tm1Mom}*/J) mice were from The Jackson Laboratory (Bar Harbor, ME). Mice were used between 2–5 months of age and were housed under specific pathogen-free conditions. *S. pneumoniae* challenges were performed in a conventional animal facility. All studies and procedures were approved by the Duke University Animal Care and Use Committee.

Antibodies and Immunoflourescence Analysis

Biotinylated- or fluorochrome-conjugated antibodies and secondary detection reagents used included: anti-mouse IgM or IgD

(Southern Biotechnology Associates, Inc., Birmingham, AL); anti-human CD19 (B4, Beckman Coulter, Miami, FL); or antibodies reactive with mouse CD21 (7G6), CD19 (ID3), B220 (RA3-6B2), CD23 (B3B4), CD5 (53-7.3), CD1d (1B1), and phycoerythrin (PE)- and cychrome-conjugated streptavidin (all from BD-PharMingen). Single cell lymphocyte suspensions from spleen and peritoneal cavity were isolated and stained at 4°C for 25 min. Cells were analyzed using a FACScan flow cytometer (Becton Dickinson, San Jose, CA), with positive and negative cell populations determined using unreactive isotype-matched antibodies (BD-Pharmingen).

Analysis of serum antibody binding to *S. pneumoniae* was carried out by incubating heat-killed bacteria (10^7 cfu) with serum diluted in PBS for 30 min at room temperature, washing with PBS, and detecting bound antibodies using PE-conjugated goat anti-mouse immunoglobulin antibodies (Southern Biotechnology Associates). 30,000 events were collected and analyzed per sample on a FACScan flow cytometer.

Immunizations and *S. pneumoniae* Infections

All infections and whole bacteria immunizations used WU2, a type 3 strain of *S. pneumoniae*, as previously described (Haas et al., 2002). For i.p. infections, bacteria were diluted in 200 μl sterile PBS with the number of cfus reconfirmed. Mice were immunized i.p. with 0.5 μg of PPS-3 (American Type Culture Collection, Rockville, MD) or heat-killed (10^7 cfu) *S. pneumoniae* in PBS (Haas et al., 2002).

Enzyme-Linked Immunosorbent Assays

Enzyme-linked immunosorbent assays (ELISAs) used AP-conjugated polyclonal goat anti-mouse IgM and IgG3 antibodies (Southern Biotechnology Associates). PPS-3-specific and PC-specific antibody titers were measured by adding serum samples to plates coated with 10 μg/ml PPS-3 in PBS or PC-BSA (Biosearch Technologies, Novato, CA) in 0.1 M borate-buffered saline overnight at 4°C. ELISAs to detect *S. pneumoniae*-specific antibody were performed as previously described (Haas et al., 2002). Endpoint titers were determined using 3-fold serial serum dilutions and measured as the reciprocal dilution yielding an OD_{405} value that was 3-fold higher than that of the negative control OD with sera omitted.

Immunohistochemistry

Frozen spleen sections (5 μm) mounted on gelatin-coated slides were fixed in acetone, rehydrated in PBS, blocked in 5% normal rabbit serum/2% bovine calf serum in PBS and reacted with biotinylated CD23 antibody (BD-Pharmingen) in 2% bovine calf serum in PBS. Sections were washed and incubated with streptavidin-HRP (Southern Biotechnology Associates) and developed with 3, 3′-diaminobenzidine substrate (Vector Laboratories, Burlingame, CA). AP-conjugated goat anti-mouse IgM antibody (Southern Biotechnology Associates) was used in conjunction with Vector blue AP substrate kit (Vector Laboratories). Fluorescence immunohistochemistry was performed following the acetone fix and blocking steps as described above. Sections were incubated with PE-conjugated anti-CD1d and FITC-conjugated anti-B220, washed, and analyzed using a fluorescence microscope.

Cell Sorting and Adoptive Transfers

B cell subsets were purified from peritoneal cavity or spleen lymphocytes using a FACSVantage SE flow cytometer (Becton-Dickinson) with purities of ~85%–95%. Alternatively, spleen or lymph node cell suspensions were enriched for B cells by Thy1.2-magnetic bead (Dynal, Lake Success, NY) depletion of T cells, with B cell purities ≥90%. After isolation, the cells were immediately transferred i.p. or i.v. into hCD19Tg or $Rag1^{-/-}$ mice.

Statistical Analysis

Data are shown as means ± SEM. Differences between sample means were assessed using Student's t test. Differences in survival were assessed using Fisher's exact test and Chi-square analysis.

Acknowledgments

We thank Dr. David Briles for helping us establish the *S. pneumoniae* system. These studies were supported by NIH grants CA96547, CA105001, and AI56363 and a grant from The Arthritis Foundation. T.F.T. is a consultant for Cellective Therapeutics. K.M.H. was supported in part by grants from the Lymphoma Research Foundation and the Leukemia & Lymphoma Society.

Received: November 20, 2004
Revised: April 15, 2005
Accepted: April 20, 2005
Published: July 26, 2005

References

Alugupalli, K.R., Leong, J.M., Woodland, R.T., Muramatsu, M., Honjo, T., and Gerstein, R.M. (2004). B1b lymphocytes confer T cell-independent long-lasting immunity. Immunity *21*, 379–390.

Amsbaugh, D.F., Hansen, C.T., Prescott, B., Stashak, P.W., Barthold, D.R., and Baker, P.J. (1972). Genetic control of the antibody response to type 3 pneumococcal polysaccharide in mice. I. Evidence that an X-linked gene plays a decisive role in determining responsiveness. J. Exp. Med. *136*, 931–949.

Antall, P.M., Meyerson, H., Kaplan, D., Venglarcik, J., and Hostoffer, R.W. (1999). Selective antipolysaccharide antibody deficiency associated with peripheral blood CD5+ B-cell predominance. J. Allergy Clin. Immunol. *103*, 637–641.

Baumgarth, N., Herman, O.C., Jager, G.C., Brown, L., and Herzenberg, L.A. (1999). Innate and acquired humoral immunities to influenza virus are mediated by distinct arms of the immune system. Proc. Natl. Acad. Sci. USA *96*, 2250–2255.

Berland, R., and Wortis, H.H. (2002). Origins and functions of B-1 cells with notes on the role of CD5. Annu. Rev. Immunol. *20*, 253–300.

Bhat, N.M., Kantor, A.B., Bieber, M.M., Stall, A.M., Herzenberg, L.A., and Teng, N.N. (1992). The ontogeny and functional characteristics of human B-1 ($CD5^+$ B) cells. Int. Immunol. *4*, 243–252.

Briles, D.E., Nahm, M., Schroer, K., Davie, J., Baker, P., Kearney, J., and Barletta, R. (1981). Antiphosphocholine antibodies found in normal mouse serum are protective against intravenous infection with type 3 *Streptococcus pneumoniae*. J. Exp. Med. *153*, 694–705.

Engel, P., Zhou, L.-J., Ord, D.C., Sato, S., Koller, B., and Tedder, T.F. (1995). Abnormal B lymphocyte development, activation and differentiation in mice that lack or overexpress the CD19 signal transduction molecule. Immunity *3*, 39–50.

Haas, K.M., Hasegawa, M., Steeber, D.A., Poe, J.C., Zabel, M.D., Bock, C.B., Karp, D.R., Briles, D.E., Weis, J.H., and Tedder, T.F. (2002). Complement receptors CD21/35 link innate and protective immunity during *Streptococcus pneumoniae* infection by regulating IgG3 antibody responses. Immunity *17*, 713–723.

Hardy, R.R., and Hayakawa, K. (2001). B cell development pathways. Annu. Rev. Immunol. *19*, 595–621.

Herzenberg, L.A. (2000). B-1 cells: the lineage question revisited. Immunol. Rev. *175*, 9–22.

Inaoki, M., Sato, S., Weintraub, B.C., Goodnow, C.C., and Tedder, T.F. (1997). CD19-regulated signaling thresholds control peripheral tolerance and autoantibody production in B lymphocytes. J. Exp. Med. *186*, 1923–1931.

Kenny, J.J., Yaffe, L.J., Ahmed, A., and Metcalf, E.S. (1983). Contribution of Lyb 5+ and Lyb 5– B cells to the primary and secondary phosphocholine-specific antibody response. J. Immunol. *130*, 2574–2579.

Krop, I., Shaffer, A.L., Fearon, D.T., and Schlissel, M.S. (1996). The signaling activity of murine CD19 is regulated during B cell development. J. Immunol. *157*, 48–56.

Makowska, A., Faizunnessa, N.N., Anderson, P., Midtvedt, T., and Cardell, S. (1999). $CD1^{high}$ B cells: a population of mixed origin. Eur. J. Immunol. *29*, 3285–3294.

Martin, F., and Kearney, J.F. (2000). B-cell subsets and the mature preimmune repertoire. Marginal zone and B1 B cells as part of a "natural immune memory". Immunol. Rev. *175*, 70–79.

Martin, F., Oliver, A.M., and Kearney, J.F. (2001). Marginal zone and

B1 B cells unite in the early response against T-7independent blood-borne particulate antigens. Immunity *14*, 617–629.

Masmoudi, H., Mota-Santos, T., Huetz, F., Coutinho, A., and Cazenave, P.A. (1990). All T15 Id-positive antibodies (but not the majority of VHT15+ antibodies) are produced by peritoneal $CD5^+$ B lymphocytes. Int. Immunol. *2*, 515–520.

Mi, Q.S., Zhou, L., Schulze, D.H., Fischer, R.T., Lustig, A., Rezanka, L.J., Donovan, D.M., Longo, D.L., and Kenny, J.J. (2000). Highly reduced protection against *Streptococcus pneumoniae* after deletion of a single heavy chain gene in mouse. Proc. Natl. Acad. Sci. USA *97*, 6031–6036.

Mond, J.J., Lees, A., and Snapper, C.M. (1995). T cell-independent antigens type 2. Annu. Rev. Immunol. *13*, 655–692.

Ohdan, H., Swenson, K.G., Kruger Gray, H.S., Yang, Y., Xu, Y., Thall, A.D., and Sykes, M. (2000). Mac-1-negative B-1b phenotype of natural antibody-producing cells, including those responding to Galα1,3-Gal epitopes in α1,3-galactosyltransferase-deficient mice. J. Immunol. *165*, 5518–5529.

Ortqvist, A. (2001). Pneumococcal vaccination: current and future issues. Eur. Respir. J. *18*, 184–195.

Rickert, R.C., Rajewsky, K., and Roes, J. (1995). Impairment of T-cell-dependent B-cell responses and B-1 cell development in CD19-deficient mice. Nature *376*, 352–355.

Sato, S., Steeber, D.A., and Tedder, T.F. (1995). The CD19 signal transduction molecule is a response regulator of B-lymphocyte differentiation. Proc. Natl. Acad. Sci. USA *92*, 11558–11562.

Sato, S., Ono, N., Steeber, D.A., Pisetsky, D.S., and Tedder, T.F. (1996). CD19 regulates B lymphocyte signaling thresholds critical for the development of B-1 lineage cells and autoimmunity. J. Immunol. *157*, 4371–4378.

Sato, S., Steeber, D.A., Jansen, P.J., and Tedder, T.F. (1997). CD19 expression levels regulate B lymphocyte development: human CD19 restores normal function in mice lacking endogenous CD19. J. Immunol. *158*, 4662–4669.

Sen, G., Wu, H.J., Bikah, G., Venkataraman, C., Robertson, D.A., Snow, E.C., and Bondada, S. (2002). Defective CD19-dependent signaling in B-1a and B-1b B lymphocyte subpopulations. Mol. Immunol. *39*, 57–68.

Wang, Y., Brooks, S.R., Li, X., Anzelon, A.N., Rickert, R.C., and Carter, R.H. (2002). The physiologic role of CD19 cytoplasmic tyrosines. Immunity *17*, 501–514.

Wardemann, H., Boehm, T., Dear, N., and Carsetti, R. (2002). B-1a B cells that link the innate and adaptive immune responses are lacking in the absence of the spleen. J. Exp. Med. *195*, 771–780.

Wuorimaa, T., and Kayhty, H. (2002). Current state of pneumococcal vaccines. Scand. J. Immunol. *56*, 111–129.

Zhou, L.-J., Smith, H.M., Waldschmidt, T.J., Schwarting, R., Daley, J., and Tedder, T.F. (1994). Tissue-specific expression of the human CD19 gene in transgenic mice inhibits antigen-independent B lymphocyte development. Mol. Cell. Biol. *14*, 3884–3894.